Neutron and X-ray Scattering Studies of Rb_2CoCl_4 and Successive Phase Transition in A_2BX_4-type Crystals

Hirotake Shigematsu[1]*, Katsura Nishiyama[2],
Yukihiko Kawamura[3], and Hiroyuki Mashiyama[4]

[1] *Faculty of Education, Yamaguchi University, Yamaguchi 753-8513, Japan*

[2] *Faculty of Education, Shimane University, Matsue 690-8504, Japan*

[3] *Comprehensive Research Organization for Science and Society, IQBRC Bldg, Tokai, Naka, Ibaraki 319-1106, Japan*

[4] *Department of Physics, Faculty of Science, Yamaguchi University, Yamaguchi 753-8512, Japan*

The soft phonon modes, which are related to the normal-incommensurate phase transition at $T_i = 294$ K and the lowest-temperature phase transition at $T_3 = 66$ K in Rb_2CoCl_4, have been measured by inelastic neutron scattering. For the normal-incommensurate phase transition, the phonon dispersion curves have been determined in the low-temperature commensurate phases, and the phase mode has been observed far below T_i. The soft mode is fully overdamped above T_i. Moreover, another soft phonon mode, which contributes to the phase transition at T_3, has been observed. Furthermore, the space group of the lowest phase is directly confirmed to be $C1c1$ by verifying extinction rules of X-ray diffraction. It has been recognized that the ratio of the ionic radius of A^+ to the average bond length B−X in the tetrahedral BX_4^{2-} ion can control the phase transition sequence. Rb_2CoCl_4 belongs to the group in which this ratio is in the range from 0.69 to 0.85, and the transition temperature decreases loosely with increasing the lattice parameter ratio c_0/a_0, where a_0 and c_0 are the lattice parameters of the normal phase.

1. Introduction

Rubidium tetrachlorocobaltate, Rb_2CoCl_4, belongs to a family of A_2BX_4-type crystals with the β-K_2SO_4 type structure such as Rb_2ZnCl_4.[1–4] Three phase transitions are observed at temperatures $T_i = 294$ K, $T_C = 192$ K, and $T_3 = 66$ K. The observed phases are summarized as follows: phase I ($T > T_i$, normal phase, space group: $Pmcn$, $Z = 4$, a_0, b_0, c_0), phase II ($T_i > T > T_C$, incommensurate phase, a_0, b_0, ~$3c_0$), phase III ($T_C > T > T_3$, $P2_1cn$, $Z = 12$, a_0, b_0, $3c_0$), and phase IV ($T < T_3$, $C1c1$, $Z = 48$, $2a_0$, $2b_0$, $3c_0$), where a_0, b_0, and c_0 are the lattice parameters of phase I. An extra anomaly of the dielectric constant has been observed at 20 K recently.[4]

Among the A_2BX_4-type crystals, the soft phonon mode was observed clearly in K_2SeO_4 both above and below the normal-incommensurate (N-INC) phase transition point by inelastic neutron scattering.[5, 6] That is to say, the transition type of K_2SeO_4 is interpreted as a displacive one. On the other hand, the soft mode above the N-INC transition temperature was not observed in Rb_2ZnBr_4,[7] Rb_2ZnCl_4,[8] or K_2ZnCl_4.[9] Therefore, it has been considered that the transition type is an order-disorder one. However, the Raman active modes were observed to soften below the N-INC transition point.[10–14] According to this evidence, it was assumed that a crossover between the displacive and the order-disorder regions occurred.[9,13,14]

An empirical law between the pressure coefficient dT/dp of transition temperature and the mechanisms of the ferroelectric phase transition has been pointed out by Samara.[15] For example, displacive type transitions in ABO_3 perovskite crystals have a negative coefficient, Whereas order-disorder type transitions in TGS, Rochelle salt, and KNO_3 have a positive coefficient.[15] Furthermore, Gesi discussed the relationship between the N-INC phase transition temperature T_i and the pressure coefficient for various A_2BX_4-type crystals with the β-K_2SO_4 type structure.[3] According to his proposition, the change in the pressure coefficient dT_i/dp with increasing T_i was related to the transition mechanism. An underdamped soft mode was observed in K_2SeO_4, which has the lowest T_i (= 130 K) among the A_2BX_4-type crystals and a negative pressure coefficient of -73 K/GPa.[16] Furthermore, the soft modes in K_2SeO_4 showed strong hardening below T_i, and the scattering intensity of the soft mode increased rapidly with decreasing temperature.[17] On the other hand, in Rb_2ZnCl_4 ($T_i = 302$ K, $dT_i/dp = 3.5$ K/GPa), Rb_2ZnBr_4 (347 K, 58 K/GPa), and K_2ZnCl_4 (553 K, 110 K/GPa), which have positive coefficients,[18,19] well-defined soft modes have not been observed in the normal phase.[7–9] The soft modes showed weak hardening far below T_i in these compounds. Thus, the order-disorder nature becomes remarkable as the transition temperature T_i increases, which has been considered to be related to the effective potential of the librational motion of the BX_4

tetrahedron.[20]

In Rb_2CoCl_4, the pressure coefficient is -12 K/GPa, which is rather small and negative.[3] Therefore, we expect that the underdamped soft modes will be observed in the normal phase, which will provide additional information about the N-INC phase transition. Incidentally, two low-energy modes, which were dependent on temperature, were observed below T_i by Raman scattering.[2] However, the phase mode was not yet observed because of the low-frequency limit of the measurements and no measurement below 90 K. In addition, the behavior of phonon modes above T_i has not been reported.

In this paper, we will report on the soft mode behavior in Rb_2CoCl_4 examined by the inelastic neutron scattering technique. The soft modes are measured in order to clarify the mechanism of the N-INC phase transition at T_i and to characterize the phase III - phase IV transition at T_3. The change in extinction rules of low-temperature phases is investigated by X-ray scattering, because some of the A_2BX_4-type crystals, Rb_2ZnBr_4[21] and Rb_2CoBr_4,[22] undergo another type of phase transition from a ferroelectric phase III to a rare phase IV. Incidentally, the extra extinction rule, which is explained by elements of extra symmetry operations, exists in phase IV of Rb_2ZnBr_4 and Rb_2CoBr_4. Finally, the relationships between the N-INC phase transition and the crystal character are discussed in the final section from the viewpoints of the ratio of the ionic radius of A^+ to the average bond length $B-X$ in the tetrahedral BX_4^{2-} ion, and the ratio between the lattice parameters a_0, b_0, and c_0.

2. Experimental

Single crystals of Rb_2CoCl_4 were grown by the Bridgman method from melt.[23,24] The starting materials were commercial powders of RbCl of 99% purity and $CoCl_2$ of 99.9% purity supplied by Soekawa Chemicals Co., Ltd. The obtained crystals were cobalt blue in color and transparent and showed poor cleavage perpendicular to the b-axis.

In order to investigate a soft phonon mode, that contributes to the N-INC phase transition, triple-axis spectrometers C1-1 and 4G, installed in the guide hall and reactor hall, respectively, at the JRR-3M reactor of the Japan Atomic Energy Research Institute (JAERI), Tokai, were used for neutron scattering. In the C1-1 spectrometer, energy scans were carried out with a fixed incident neutron beam of $k_i = 1.55$ Å^{-1} with a pyrolytic graphite PG002 monochromator and a PG002 analyzer for obtaining high-energy resolution. These systems were employed for measuring low-energy excitations below 3 meV. In the 4G spectrometer, a fixed incident neutron beam of $k_i = 2.664$ Å^{-1} was used for measuring high-angle reflections and

high-energy excitations. The used conditions were the following: PG002 monochromator, PG002 analyzer, PG filter, and 40'-40'-40'-40' collimation. On the other hand, in order to investigate the soft phonon mode, which contributes to the phase III - phase IV transition, a triple-axis spectrometer T1-1 installed in the guide hall at JAERI was used. The used conditions were the following: an incident beam of k_i = 2.558 Å^{-1}, PG002 monochromator, PG002 analyzer, PG filter, and open-40'-60'-60' collimation. In all spectrometers, a crystal of about 3 cm^3 size was mounted in an aluminum can filled with helium gas and set in a closed-cycle refrigerator that was cooled by cryogenics below room temperature, or in an electric furnace for measuring above room temperature. Data were collected in the (a^*, c^*) or (a^*, b^*) scattering plane, and the measurements of phonon dispersion were performed along the line 200-202 for C1-1, the lines 200 - 202 and 400 - 402 for 4G, and the lines 420 - 510 and 360 - 270 for T1-1.

The X-ray diffraction measurements were performed by using a four-circle diffractometer (Huber 422+511.1) attached to a rotating-anode-type generator (Rigaku RU-300) with an X-ray power of 50 kV × 150 mA. For the investigation of extinction rules and the measurements of peak intensities, the incident beam (Mo-Kα) was monochromated by pyrolytic graphite (HOPG) to increase the reflection intensity.

3. Results

Figure 1 shows the results of typical energy scans with constant Q at $20\frac{4}{3}$ well below the N-INC phase transition temperature T_i by the use of 4G. Two modes are observed as indicated by arrows at 10 K. One is a temperature-independent 4.7 meV mode, which is interpreted to be an optical mode characterized by the zone folding back of the dispersion.[6] Another peak observed clearly below 80 K is a temperature-dependent mode, which is recognized as the phase mode from the behavior of dispersion.[6,14] The observed phonon peaks except for the quasi-elastic scattering were fitted to two Lorentzian-type cross sections convoluted with the instrumental resolution function. On the other hand, neither the amplitude mode nor another soft mode was observed in our study.[2,10-14] The temperature dependences of observed mode energies at $20\frac{4}{3}$ are shown in Fig. 2. Full circles and full triangles are neutron data points for phase and 4.7 meV modes, respectively. Furthermore, open circles show the Raman spectra for a totally symmetric mode, which corresponds to the amplitude mode reported previously.[2] This figure indicates that the phase mode is underdamped in the low-temperature region.

The phonon dispersion curves are shown in Fig. 3 in an extended zone scheme along the (0

$0\ \xi$) direction at 10 K, 20ξ: $0 \le \xi < \frac{1}{3}$, $202\text{-}\xi$: $\frac{1}{3} \le \xi < \frac{2}{3}$, and 20ξ: $\frac{2}{3} \le \xi < 1$ by the use of 4G and C1-1.[6] In the vicinity of $\xi = \frac{2}{3}$, the phase mode and TA branches are clearly observed, because the $\xi = \frac{2}{3}$ point becomes equivalent to a Γ point, and the reflections $20\frac{2}{3}$ and $20\frac{4}{3}$ are strong superlattice reflections below T_C. Although it is expected that the dispersion curves in the periodic zone scheme should be periodic,[6] some parts of branches were so broad and weak that it was difficult to observe the whole branches. In Fig. 3, the clearly observed peaks are plotted.

Figure 4 shows the phonon dispersion curves along the $(0\ 0\ \xi)$ direction in the normal phase. Although the behavior of the phonon dispersion was clearly observed, no softening of the branch was observed at approximately $\xi = \frac{2}{3}$, where the softening was reported in the case of K_2SeO_4.[5] Furthermore, we could not observe the anticrossing of the acoustic branch with an optic one in Fig. 4. With increasing temperature, the slope of the branch decreases slightly, indicating the decrease in the elastic constant as the crystal approaches the melting point. The remarkable quasi-elastic diffuse scattering at approximately $\xi = \frac{2}{3}$ was also observed in the normal phase of Rb_2CoCl_4 and it is similar to that of Rb_2ZnBr_4.[14]

Figure 5 shows the phonon dispersion curves in an extended-zone scheme along the $(\xi\ \xi\ 0)$ direction above the phase transition temperature $T_3 = 66$ K. A transverse optic mode is degenerate with a transverse acoustic branch at the zone-boundary S point, $\xi = \frac{1}{2}$. It is clear that this mode softens in the vicinity of the S point with decreasing temperature. However, it was difficult to observe the mode below T_3 because the mode became so broad and weak around the S point.

Figure 6 shows the temperature dependence on cooling of the integrated intensities I of the superlattice reflections $20\frac{20}{3}+\delta$ and $\frac{1}{2}\frac{17}{2}0$, and the Bragg reflection 180 determined by X-ray scattering experiments, where indices are referred to the normal phase. The temperature dependence of I can be fitted to the relation

$$I \propto \left(T_i - T\right)^{2\beta} \quad \text{or} \quad I \propto \left(T_3 - T\right)^{2\beta}. \tag{1}$$

The fitted relation is shown by a solid line. The values of critical exponent β are 0.40 for the $20\frac{20}{3}+\delta$ reflection, 0.33 for the $\frac{1}{2}\frac{17}{2}0$ reflection, and 0.43 for the 180 reflection. These critical exponents β are not close to the mean field value of $\beta = 0.50$ but rather closer to the three-dimensional Ising exponent ($\beta = 0.33$) or critical exponent in K_2SeO_4 ($\beta = 0.40$).[5] The misfit parameter δ is about 0.02 at 290 K.[1] Although the misfit parameter δ decreased to zero

discontinuously at the look-in temperature T_C, the integrated intensity increases continuously. Note that the angles α, β, and γ were 90° within the experimental error in phase IV, and we did not recognize any thermal hysteresis between the heating and cooling processes. Although a slight dielectric anomaly was reported at 20 K,[4] no anomaly of the intensity distribution nor change of extinction rules was found at approximately 20 K in this study.

4. Discussion

4.1 Structures and phase transitions in Rb₂CoCl₄

The phase mode of Rb_2CoCl_4 was observed clearly on the (a^*, c^*) scattering plane in the low-temperature commensurate phases by the inelastic neutron scattering, compared with the cases of Rb_2ZnBr_4[14] and Rb_2ZnCl_4.[8] On the other hand, the amplitude mode, which was already reported as the Raman spectra for $a(cc)b$ and $b(aa)c$ geometries,[2] was not detected in Rb_2CoCl_4. Furthermore, the softening of an optic branch was not observed at high temperatures above T_i, and the soft mode was fully overdamped above the N-INC phase transition. These inelastic neutron scattering measurements reveal that the behaviors of phonon modes both above and below the N-INC phase transition point of Rb_2CoCl_4 were similar to those of Rb_2ZnCl_4, Rb_2ZnBr_4, and K_2ZnCl_4. Although the pressure coefficient dT_i/dp of Rb_2CoCl_4 is small but negative like that of K_2SeO_4, the order-disorder nature appears remarkably. [3]

In the (a^*, b^*) scattering plane, the frequencies of the degenerate mode, which contribute to the phase transition, tends to zero upon approaching T_3. Although we could not observe clear modes around the S point below T_3, we can predict the existence of two modes as in the case of Rb_2ZnBr_4.[21]

The Bragg reflections at the position $hk0$: $h+k = 2n+1$ in Rb_2ZnBr_4 and Rb_2CoBr_4 did not appear below T_3. However, these Bragg reflections appear in Rb_2CoCl_4, and their intensities increase with decreasing temperature.[21,22] Therefore, the following extinction rules are confirmed in phase IV: reflections h_s0l_s and $h_sk_sl_s$ are absent when $l_s = 2n+1$ and $h_s+k_s = 2n+1$, respectively, under the $2a_0 \times 2b_0 \times 3c_0$ superlattice cell, where the Miller indices h_s, k_s, and l_s are referred to the superlattice cell. From group theoretical considerations, Dvorak and Kind showed that three space groups, $P11b$, $C1c1$, and $P1$, are possible for such cases.[25] The space group of phase IV is $C1c1$ with $Z = 48$, considering the observed extinction rules and the existence of spontaneous polarization.[2,4,25] It was found that Rb_2CoCl_4 undergoes the same series of successive phase transitions as many A_2BX_4-type ferroelectrics such as Rb_2ZnCl_4, K_2ZnCl_4, and K_2CoCl_4.

Important results of the lattice dynamics calculations are follows: in all cases, the unstable or soft phonon branch is either optical or the results of the anticrossing of an optical branch with an acoustic one takes place.[26,27] Indeed, in the case of K_2SeO_4, the clear softening of the Λ_2 branch causes the anticrossing of the acoustic branch with an optical one, the unstable or soft branch being essentially the prolongation of the lowest Λ_2-Λ_3 optical branch.[5,6] Furthermore, the behaviors of the lowest Λ_2-Λ_3 optical branches of Rb_2SeO_4 and K_2CrO_4 are similar to those of K_2SeO_4, where the mode softens slightly with decreasing temperature, although the frequency remains finite at very low temperatures.[28–30] In the case of Rb_2CoCl_4, we could not observe either the anticrossing or the softening above T_i (see Fig. 4).

4.2 Grouping of A_2BX_4-type crystals

It has been reported that many of the A_2BX_4-type crystals have the β-K_2SO_4 type structure at high temperatures. However, these crystals do not necessarily undergo the same succession of phase transitions. It has been recognized that the ionic radius of A^+, $r(A)$, and the average bond length B−X in the tetrahedral BX_4^{2-} ion, $r(BX)$, can control the phase transition sequence.[31,32] A_2BX_4-type crystals can be loosely classified into three main groups from the ratio

$$\rho = r(A)/r(BX) \qquad\qquad (2)$$

as follows.

The grouping of A_2BX_4-type crystals with important parameters is shown in Table I.

Group I.   When the ratio ρ is below 0.69, the Sr_2GeS_4-type structure (space group $P2_1/m$) in the α-sequence is stable, and many compounds with relatively large ratios perform α-β transitions, for example, K_2ZnBr_4, K_2CoBr_4, and Rb_2ZnI_4.[31,32] These compounds take the β-K_2SO_4 type structures in the β-sequence at high temperatures.

Group II.   When the ratio ρ is less than 0.85 beyond 0.69, all compounds have the normal phase (space group $Pmcn$) as the highest-temperature phase. In addition, it is divided into the following two groups.

Group II-a.   As the temperature decreases, the compounds transform into the threefold-modulated ferroelectric phase (space group $P2_1cn$) via the incommensurate phase with modulation along the c-axis. Typical compounds are Rb_2ZnCl_4, Rb_2ZnBr_4, and K_2ZnCl_4. Rb_2CoCl_4 also belongs to group II-a.

Group II-b.   As the temperature decreases, the compounds transform into the different

successive phase transitions, and the structures of each phase are not the same in contrast to those of the compounds that belong to group II-a. Here, the transition temperature at phases I – to - II is denoted as $T_{I\text{-}II}$. Furthermore, some compounds have no transition and retain the orthorhombic structure (space group $Pmcn$) down to 0 K. Typical compounds in group II-b are Cs_2ZnCl_4, Cs_2ZnI_4, and Cs_2CdBr_4.

Group III. When the ratio ρ is more than 0.85, all compounds have the hexagonal structure (α-K_2SO_4 type structure, space group $P6_3/mmc$) in the highest-temperature phase. All A_2BO_4-type oxides (X = O) belong to this group. Although K_2SeO_4 and Rb_2MoO_4 have the N-INC phase transition, the other oxides retain the β-K_2SO_4 type structure down to 0 K and have a hypothetical phase transition temperature below 0 K.[27, 33)] Incidentally, a softening tendency of the Λ_2 phonon branch, which is similar to those for K_2SeO_4, was observed as evidence of the hypothetical transition in Rb_2SeO_4 and K_2CrO_4.[28-30)] It is considered that the transition corresponds to the N-INC phase transition of K_2SeO_4 and Rb_2MoO_4.

Here, the lattice parameter ratios c_0/a_0 and c_0/b_0 in phase I (space group $Pmcn$) are adopted as additional parameters for groups II and III, where the c-axis is a pseudo-hexagonal axis and $b_0 \cong \sqrt{3}\, a_0$ (See Table I). Crystals in groups II and III have the same standard structure (space group $Pmcn$) and they have almost the same ratios c_0/b_0 and c_0/a_0. Furthermore, the difference in size of the lattice parameters between groups II and III is related to the change in the slope of the TA phonon. In general, the slope at the Γ point ($\xi = 0$) is large when the lattice parameter is small. As a result, an existence of the phonon mode softening and the anticrossing are caused in this case.

According to the rigid body motion analysis and Brown theory,[34,35)] the A(1) (11-coordinated site) ion is the main one that produces the different transitions, and the rotation of the tetrahedral BX_4^{2-} ion around the a-axis is important to remain the orthorhombic structure (space group $Pmcn$). It contributes to changing the lattice parameter ratios c_0/a_0 ($\cong \sqrt{3}\, c_0/b_0$) and c_0/b_0. Figure 7 shows the relationships between lattice parameter ratios c_0/a_0 and c_0/b_0, and between the ratio c_0/a_0 and phase transition temperatures of A_2BX_4-type crystals, which belong to group II. The high-temperature normal phase (phase I) of this group has the same orthorhombic structure (space group $Pmcn$). All transition temperatures T_i, T_C, T_3, and $T_{I\text{-}II}$ decrease loosely with increasing lattice parameter ratio c_0/a_0.

Although the successive phase transitions in group II are not completely the same, it turns out that a certain rule is also generally followed. The loss of transition in some cesium compounds, Cs_2ZnBr_4, Cs_2ZnCl_4, and Cs_2CoCl_4 ($c_0/a_0 > \sim 1.32$), can therefore be explained

using the plot of the cell parameter ratio c_0/a_0 versus transition temperatures T_i and $T_{I\text{-}II}$. Recently, we have revealed that Rb_2MoO_4 is the second example that possesses the N-INC phase transition in A_2BO_4-type crystals (group III),[33] and the new phase transition is expected as a displacive-type transition with a typical soft phonon mode. Furthermore, various studies on the N-INC phase transition in Rb_2MoO_4 are now in progress.

In this report, we have confirmed the phase mode, which is related to the N-INC phase transition, in the low-temperature commensurate phase. Although we expected the existence of the underdamped soft modes in the normal phase, such softening behavior was not observed. Therefore, the mechanism responsible for the N-INC phase transition of Rb_2CoCl_4 is similar to that of Rb_2ZnCl_4, Rb_2ZnBr_4, and K_2ZnCl_4.

References

*E-mail: shigema@yamaguchi-u.ac.jp

1) H. Kasano, H. Mashiyama, K. Gesi, and K. Hasebe, J. Phys. Soc. Jpn. **56**, 831 (1987).

2) V. I. Torgashev, Yu. I. Yuzyuk, F. Smutny, P. Vanek, and B. Brezina, Phys. Status Solidi B **154**, 777 (1989).

3) K. Gesi, J. Phys. Soc. Jpn. **59**, 1841 (1990).

4) T. Yamaguchi and F. Shimizu, Ferroelectrics **217**, 129 (1998).

5) M. Iizumi, J. D. Axe, G. Shirane, and K. Shimaoka, Phys. Rev. B **15**, 4392 (1977).

6) J. D. Axe, M. Iizumi, and G. Shirane, Phys. Rev. B **22**, 3408 (1980).

7) C. J. de Pater, J. D. Axe, and R. Currat, Phys. Rev. B **19**, 4684 (1979).

8) H. Mashiyama, H. Shigematsu, K. Sugimoto, H. Kawano, Y. Oohara, and H. Yoshizawa, J. Korean Phys. Soc. (Proc. Suppl.) **27**, S98 (1994).

9) K. Gesi and M. Iizumi, J. Phys. Soc. Jpn. **53**, 4271 (1984).

10) E. Francke, M. Le Postollec, J. P. Mathieu, and H. Poulet, Solid State Commun. **35**, 183 (1980).

11) M. Takashige, T. Nakamura, M. Udagawa, S. Kojima, S. Hirotsu, and S. Sawada, J. Phys. Soc. Jpn. **48**, 150 (1980).

12) M. Wada, A. Sawada, and Y. Ishibashi, J. Phys. Soc. Jpn. **50**, 531 (1981).

13) T. Sekine, M. Takayama, K. Uchinokura, and E. Matsuura, J. Phys. Soc. Jpn. **55**, 3903 (1986).

14) H. Shigematsu, H. Mashiyama, M. Takesada, K. Ohshima, Y. Oohara, and T. Matsui, J. Phys. Soc. Jpn. **69**, 2905 (2000).

15) G. A. Samara, J. Phys. Soc. Jpn. Suppl. **28**, 399 (1970).

16) S. Kudo and T. Ikeda, J. Phys. Soc. Jpn. **50**, 733 (1981).

17) M. Wada, H. Uwe, A. Sawada, Y. Ishibashi, Y. Takagi, and T. Sakudo, J. Phys. Soc. Jpn. **43**, 544 (1977).

18) K. Gesi, Ferroelectrics **64**, 97 (1985).

19) K. Gesi, J. Phys. Soc. Jpn. **53**, 62 (1984).

20) H. Mashiyama, J. Korean Phys. Soc. **29**, S419 (1996).

21) H. Shigematsu, H. Mashiyama, Y. Oohara, and K. Ohshima, J. Phys.: Condens. Matter **10**, 5861 (1998).

22) M. Imamoto, Graduation thesis, Faculty of Scinece, Yamaguchi University, Yamaguchi (1999) [in Japanese].

23) K. Gesi, J. Phys. Soc. Jpn. **54**, 2401 (1985).

24) F. Shimizu, H. Suzuki, T. Yamaguchi, and S. Sawada, J. Phys. Soc. Jpn. **57**, 1466 (1988).

25) V. Dovorak and R. Kind, Phys. Status Solidi B **107**, K109 (1981).

26) I. Etxebarria, J. M. Perez-Mato, and A. Criado, Phys. Rev B **42**, 8482 (1990).

27) I. Etxebarria, J. M. Perez-Mato, and G. Madariaga, Phys. Rev B **46**, 2764 (1992).

28) I. Etxebarria, M. Quilichini, J. M. Perez-Mato, P. Boutrouille, F. J. Zuniga, and T. Breczewski, J. Phys.: Condens. Matter **4**, 8551 (1992).

29) H. Shigematsu, Y. Akishige, H. Mashiyama, T. Tojo, H. Kawaji, T. Atake, and T. Matsui, J. Korean Phys. Soc. **46**, 235 (2005).

30) H. Shigematsu, Y. Akishige, T. Matsui, T. Tojo, H. Kawaji, and T. Atake, J. Therm. Anal. Calorim. **81**, 555 (2005).

31) H. Mashiyama, M. Takesada, M. Kojima, and H. Kasano, Ferroelectrics **152**, 313 (1994).

32) H. Kasano, S. Tsuchiyama, and H. Mashiyama, J. Korean Phys. Soc. **32**, S53 (1998).

33) H. Shigematsu, K. Nomura, K. Nishiyama, T. Tojo, H. Kawaji, T. Atake, Y. Kawamura, T. Miyoshi, Y. Matsushita, M. Tanaka, and H. Mashiyama, Ferroelectrics **414**, 195 (2011).

34) I. D. Brown, Acta Crystallogr., Sect. B **48**, 553 (1992).

35) X. Solans, C. Ruiz-Perez, C. Gonzalez-Silgo, L. Mestres, M. L. Martinez-Sarrion, and E. Bocanegra, J. Phys.: Condens. Matter **10**, 5245 (1998).

Figure captions

Fig. 1.   Neutron scattering spectra at $20\frac{4}{3}$ at 200, 100, 80, 50, 30, and 10 K. Two modes, which are indicated by arrows, are resolved: the lower-frequency peak is the phase mode, and the upper one is the temperature-independent mode.

Fig. 2.   Temperature dependence of observed mode energies at $20\frac{4}{3}$ below T_i. Fulled circles and triangles are neutron data for phase and 4.7 meV modes, respectively. Open circles show amplitude mode observed by Raman spectroscopy in Ref. 2. Solid and broken lines are just guides to the eye.

Fig. 3.   Phonon dispersion curves in an extended zone scheme along the $(0\ 0\ \xi)$ direction at 10 K in the low-temperature commensurate phase. The solid lines are guides to the eye.

Fig. 4.   Phonon dispersion curves along the $(0\ 0\ \xi)$ direction at 300, 400, and 500 K in the normal phase. A higher-frequency mode is shown at only 500 K. The solid lines are guides to the eye.

Fig. 5.   Phonon dispersion curves along the $(\xi\ \xi\ 0)$ direction above T_3. The solid lines are guides to the eye.

Fig. 6.   Temperature dependences of the integrated intensities of the superlattice reflections $20\frac{20}{3}+\delta$ and $\frac{1}{2}\frac{17}{2}0$, and the Bragg reflection 180 on cooling.

Fig. 7.   (Color online) Relationships between the lattice parameter ratios c_0/a_0 ($\cong \sqrt{3}\ c_0/b_0$) and c_0/b_0, and between the ratio c_0/a_0 and phase transition temperatures of A_2BX_4-type crystals, which belong to group II. (a) The solid line represents the hexagonal lattice metric $1/\sqrt{3}$. The dotted lines in parallel with the solid line are guides to the eye, which are drawn to cover the experimental results. (b) Only the highest transition temperature T_{I-II} is shown for Cs_2BX_4 crystals in group II-b.

Table I. Grouping of A_2BX_4-type crystals. Here, ρ (= $r(A)/r(BX)$) stands for the ratio of the ionic radius of A^+ to the average bond length $B-X$ in the tetrahedral BX_4^{2-} ion in Refs. 31 and 32. Rb_2CoCl_4 belongs to group II-a.

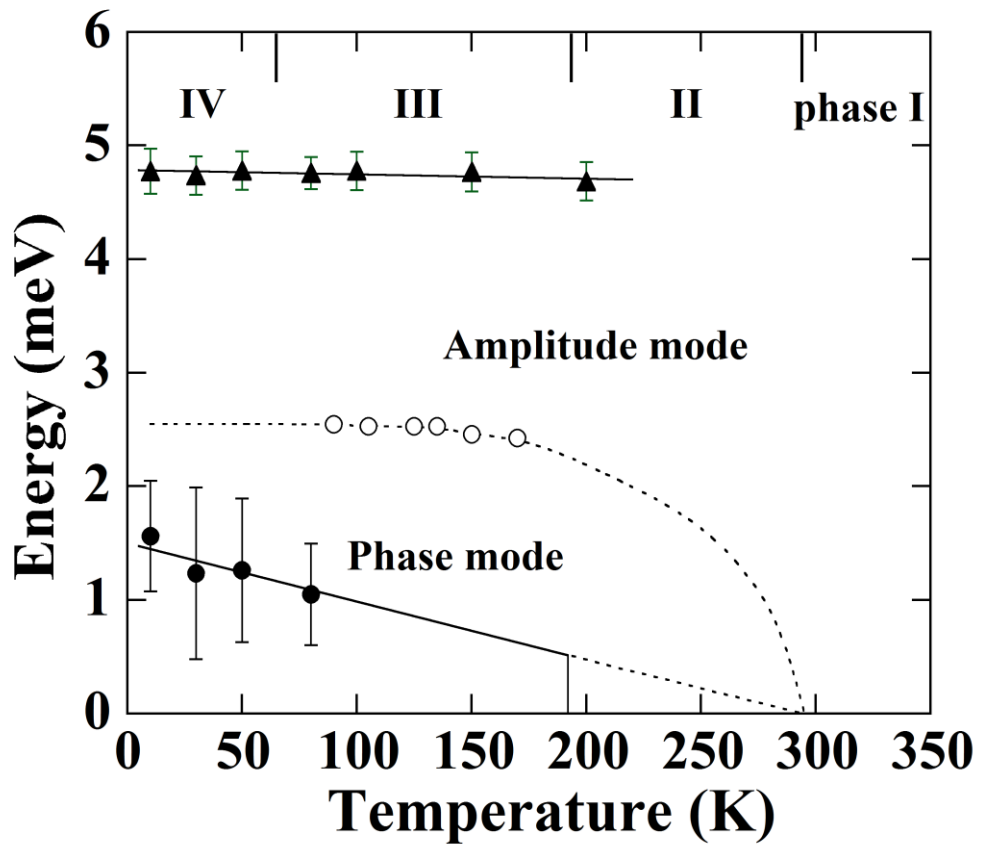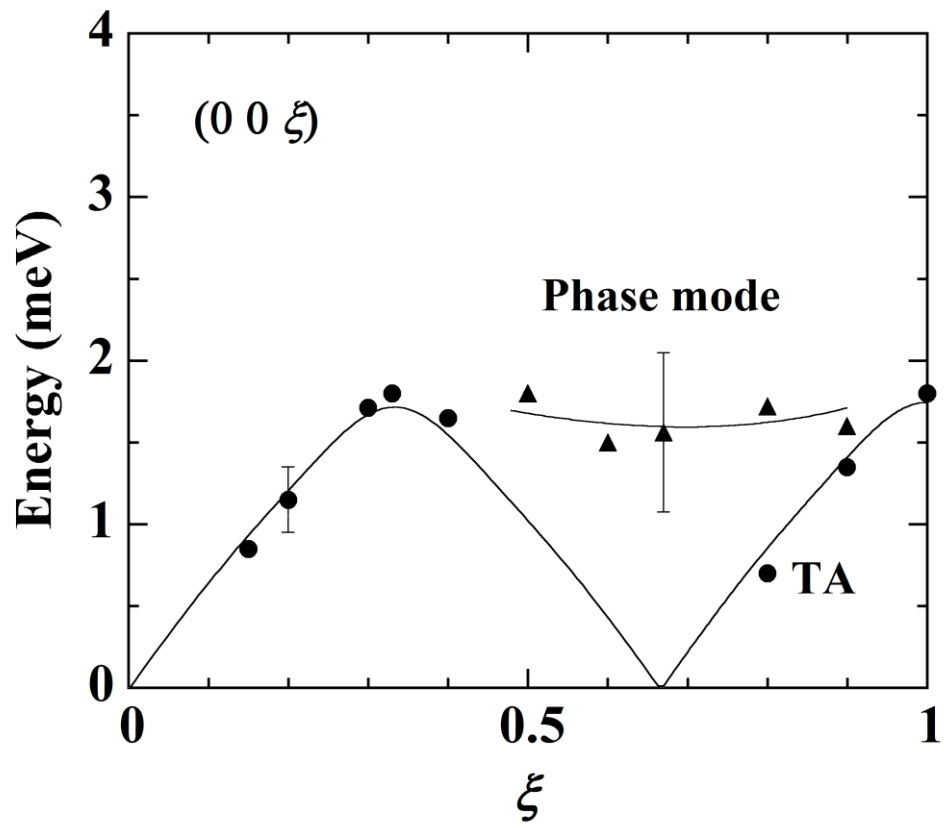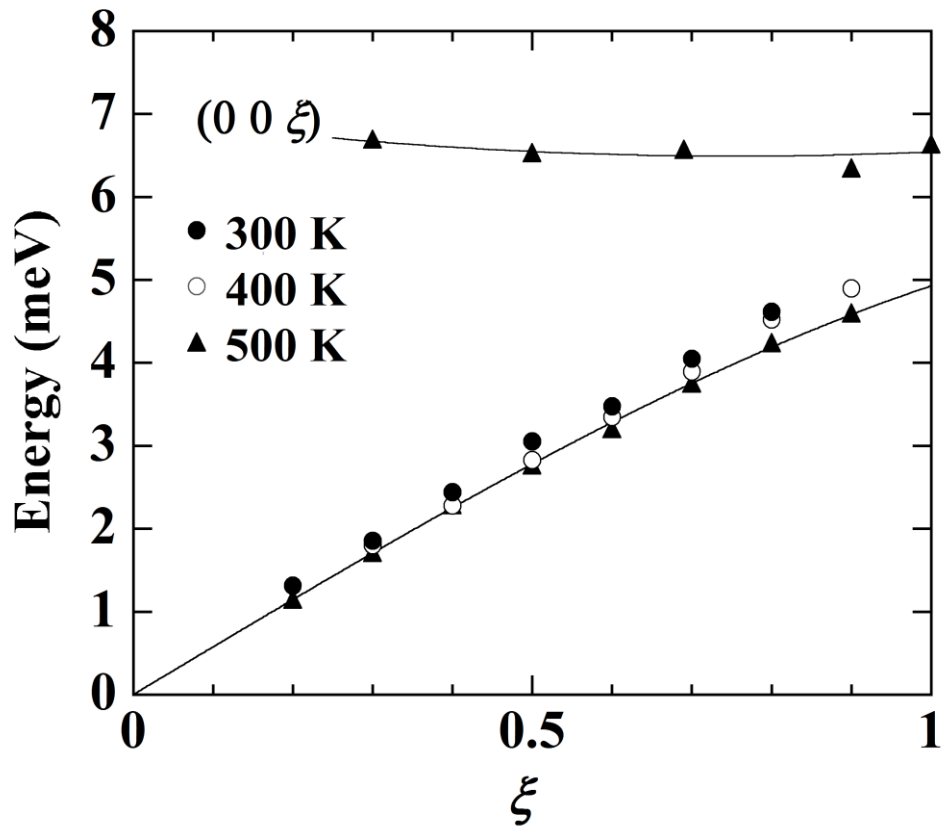| | A_2BX_4-type (X=Br, Cl, I and O) | | | |
| | $A_2BX'_4$-type (X'=Br, Cl and I) | | | A_2BO_4-type |
| Group | I | II | | III |
		II-a	II-b	
ρ	~ 0.69	0.69 ~ 0.85		0.85 ~ 1.30
c_0/a_0	−	1.23 ~ 1.28	1.28 ~ 1.33	1.26 ~ 1.34
(c_0/b_0)	−	(0.72 ~ 0.73)	(0.73 ~ 0.76)	(0.72 ~ 0.76)
a_0 [Å]	−	7.2 ~ 7.7	7.4 ~ 8.3	5.7 ~ 6.6
N-INC phase transition	No	Yes	Yes / No	Yes
Anticrossing	−	No	−	Yes
Soft mode	−	No	−	Yes
Characteristic	−	order-disorder ($T_i < T$) displacive ($T_i > T$)	−	displacive
Typical crystals	K_2ZnBr_4	Rb_2ZnCl_4	Cs_2ZnCl_4	K_2SeO_4
	K_2CoBr_4	Rb_2ZnBr_4	Cs_2ZnI_4	Rb_2MoO_4
	Rb_2ZnI_4	K_2ZnCl_4	Cs_2CdBr_4	Rb_2SeO_4
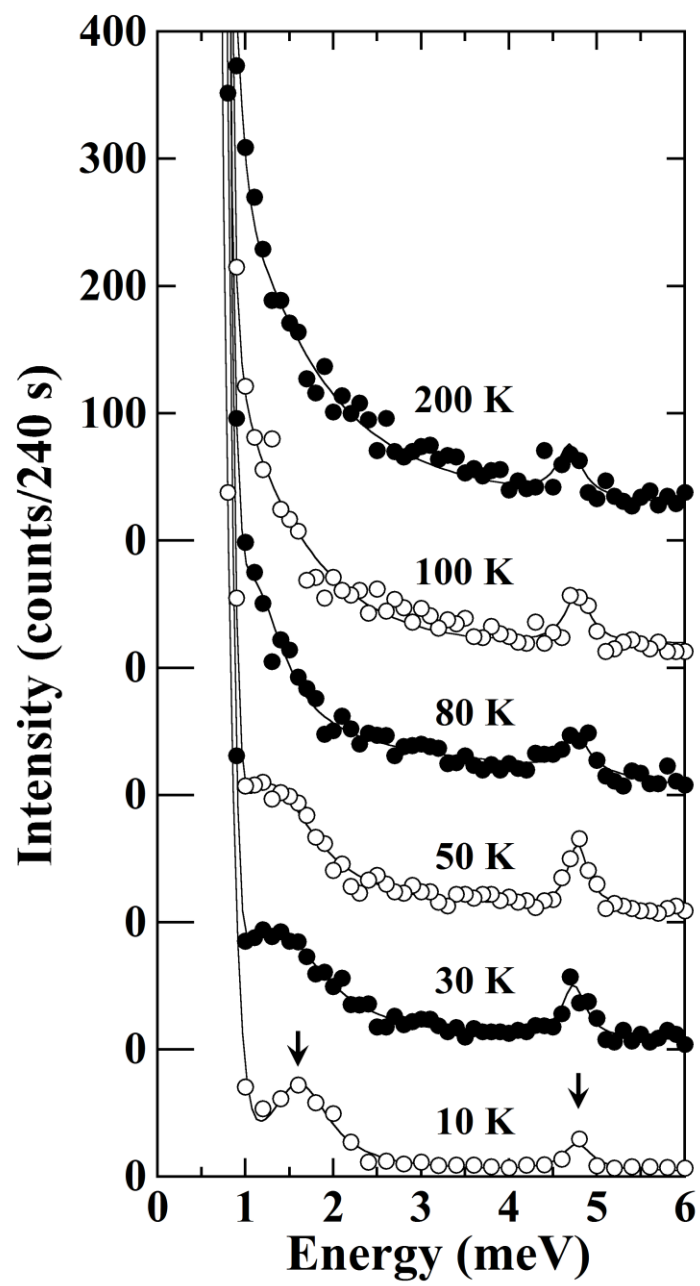
Fig. 1

Fig. 2

Fig. 3

Fig. 4

Fig. 5

Fig. 6

Fig. 7